

Flow and heat transfer over a backward-facing step with a cylinder mounted near its top corner

Hiroshi Suzuki, Sigeo Kida, Takayuki Nakamae and Kenjiro Suzuki
Department of Mechanical Engineering, Kyoto University, Kyoto, Japan

A study was made to see if it is possible to enhance the heat transfer in the downstream region of a backward-facing step, where heat transfer is normally deteriorated, by the insertion of a cylinder near the top corner of the step. Cylinder size and streamwise position of the cylinder were kept constant but the cross-stream position of the cylinder was changed in three steps. Results of the heat transfer experiment, flow visualization, and measurement of the averaged and fluctuating flow fields were reported. When the cylinder was mounted at a position, a little higher than the top surface of the step, a jet-like flow pattern emerged in the averaged velocity profile beneath the cylinder and the recirculating flow was intensified. Therefore, the velocity of recirculating flow near the wall is increased at some streamwise positions. Additionally, the velocity fluctuation was intensified not only in the shear layer between the jet-like flow and the recirculating flow regions but also in the near wall region, resulting in the effective augmentation of heat transfer in this case. Therefore, it is concluded that the mounting of a cylinder is effective in the enhancement of deteriorated heat transfer in the recirculating flow region, if it is mounted in a proper position.

Keywords: convective heat transfer; heat transfer augmentation; recirculating flow; backward-facing step; insertion of cylinder; heat transfer experiment; flow visualization; laser Doppler velocimeter

Introduction

Several studies have been made for the heat transfer downstream from a backward-facing step¹⁻⁶ and it is well known that, although high heat transfer coefficient can be attained around the flow reattachment point, heat transfer is somewhat deteriorated on the wall surface within the recirculating flow region. This lower heat transfer coefficient in that region is partly due to the lower thermal conductance between the main flow and recirculating flow region.⁶ The present study was initiated to seek to enhance the deteriorated heat transfer in the recirculating flow region.

The present authors have been doing numerical and experimental studies on a low Reynolds number, channel flow obstructed with a rod mounted in a central plane.⁷⁻⁹ In this type of periodically changing, unsteady, laminar flow, it was found that a nonzero velocity-temperature correlation is generated and that it enhances the channel wall heat transfer. This article is an application of those previous studies and deals with the case of mounting a cylinder near the top corner of the step in order to disturb an otherwise inactive recirculating flow region. The cylinder is expected to generate an unsteady pressure field synchronized with the periodical behavior of its wake, which hopefully destabilizes the recirculating flow region intermittently and yields better heat exchange between the main flow and the recirculating flow regions. In the following, the heat transfer data, the results of flow visualization, and the measured data of the averaged and fluctuating velocity components for the flow system under discussion are presented. In

this first attempt, flow Reynolds number is kept rather low, and the size and streamwise position of the cylinder are fixed. Extended study for a larger Reynolds number range and for various sizes and streamwise positions of the cylinder will be made in the near future.

Experimental apparatus and procedures

Experiments were made in a water open channel schematically illustrated in Figure 1. The bottom wall of the channel was made of opaque Bakelite plate of 5 mm thickness, but the side walls were made of transparent acrylic resin. A magnified view of the test section is shown in Figure 2 together with the descriptions of the coordinate system (x, y) and the definitions of some geometric parameters to be used in the following discussions. The cylinder size, d , and the step height, H , were kept constant in all experiments, i.e., equal to 8 and 20 mm, respectively. The normal position of the cylinder was changed in three steps, at the positions of $0.8H$, H , and $1.5H$ above the bottom wall surface, while its streamwise position was fixed at $0.6H$ downstream from the step. For brevity, the experiments for these positions will be referred to respectively as the cases C1, C2, and C3. For comparison, another experiment was made for a case when no cylinder was inserted. This will be referred to as case C0.

Step-height Reynolds number, Re , was changed in three steps, i.e., $Re = 700, 1,000, 1,400$, for the heat transfer experiments by controlling water flow rate although Re was kept constant at $Re = 1,400$ for flow visualization and velocity measurements. The cross-sectional averaged velocity at a cross section just upstream of the step was introduced as the velocity scale for the definition of Re . The fluid properties to be

Address reprint requests to Professor K. Suzuki at the Department of Mechanical Engineering, Kyoto University, Kyoto 606, Japan.

Received 18 October 1990; accepted 28 May 1991

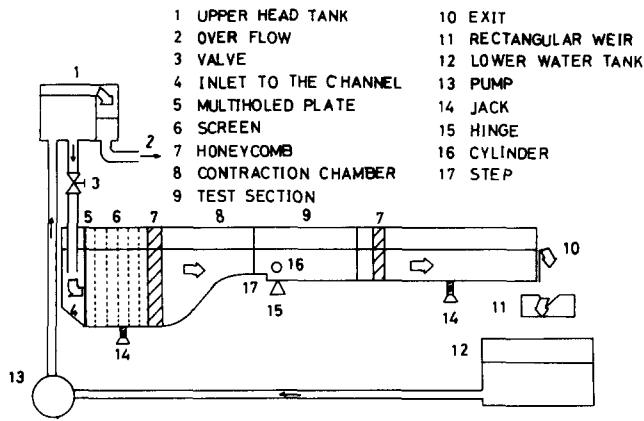


Figure 1 Experimental apparatus

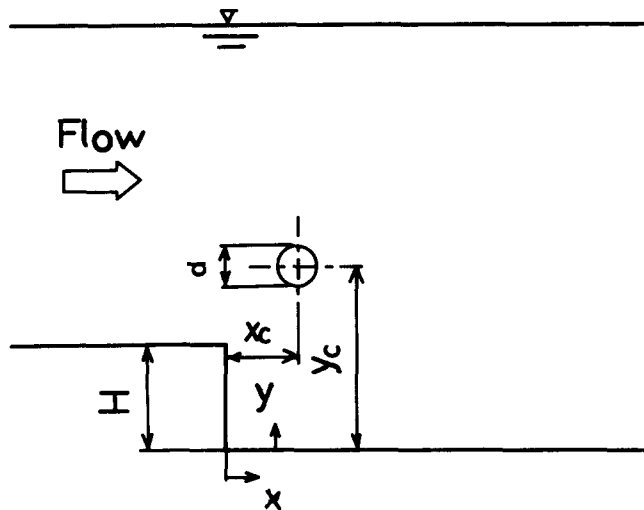


Figure 2 Test section

introduced in the Reynolds number as well as in the Nusselt number were evaluated at the temperature measured by a thermometer positioned in a calming section of the channel upstream from the test section. The corresponding water depth at the test section was about 100 mm in all experiments. In some preliminary heat transfer experiments, water depth was changed by changing the height of a weir attached to the

downstream end of the test section but keeping the step-height Reynolds number constant, and it was confirmed that the heat transfer data are free from the effect of water depth at the level of 100 mm. Thus, waves on the free surface and related unsteadiness of the flow rate, if any, were therefore concluded not to seriously affect the flow pattern near the wall and the wall heat transfer at this level of water depth.

Nine strips of stainless-steel sheets of 30 μm thickness and 48 mm width were glued on the bottom surface of the test section from 150 mm upstream of the step to 1,270 mm downstream of the step. These strips were in alignment with the streamwise direction of the flow, leaving a small gap between each other. These were heated by passing alternating electric current through them so that heating of the bottom surface was made approximately at uniform heat flux. The streamwise distribution of the surface temperature was measured with a total of 113 thermocouples attached to the back surface of the sheet glued on the centerline of the test section. Another 16 thermocouples were attached to the back surface of the other strips at two different streamwise positions. The outputs of these spanwisely allocated thermocouples agreed with each other to within 8 percent. Thus, two-dimensionality of the flow and thermal fields was confirmed to exist. Streamwise non-uniformity of wall heat flux was caused by heat leakage toward the back surface of the heated wall. The degree of nonuniformity was evaluated with an assumption that the heat leakage results from one-dimensional heat conduction through the wall and was confirmed to be inconspicuous. For the assessment of the surface temperature of the backside of the wall, another 35 thermocouples were attached to the back surface of the bottom wall. The Nusselt number, Nu_H , to be shown later is defined as follows:

$$Nu_H = \frac{q_w H}{(T_w - T_0)\lambda} \quad (1)$$

where q_w is the net local wall heat flux, T_w the local wall temperature, T_0 the inlet flow temperature, and λ is the thermal conductivity of water evaluated at the temperature T_0 .

In order to understand the background of heat transfer augmentation, flow visualization and measurements of fluctuating velocities were performed for the highest Reynolds number, i.e., $Re = 1,400$.

For flow visualization, the dye injection method was applied. Dye was injected from two thin tubes positioned at a streamwise location about 10 mm upstream from the step. They were traversed in a normal direction to establish the whole picture for the flow pattern over a wider space. Dye injection velocity

Notation		x	Streamwise distance from backward-facing step (mm)
a	Wavelength of laser light (m)	y	Normal distance from bottom wall (mm)
d	Diameter of cylinder (mm)	<i>Greek symbols</i>	
f_0	Optical shifted frequency (Hz)	θ_a, θ_b	Intersection angle (radian)
f_{DH}, f_{DV}	Doppler frequency (Hz)	λ	Thermal conductivity (W/mK)
H	Height of backward-facing step (mm)	ν	Kinematic viscosity (m ² /s)
Nu_H	Nusselt number	<i>Subscripts and superscripts</i>	
q	Heat flux (W/m ²)	m	Cross-section average
Re	Reynolds number = $U_m H / \nu$	c	Cylinder position
T	Temperature (K)	w	Wall
U	Streamwise velocity (m/s)	0	Inlet
u	Fluctuating component of streamwise velocity (m/s)	—	Time average
v	Fluctuating component of normal velocity (m/s)		Intensity
V_a, V_b	Component of velocity shown in Figure 3		

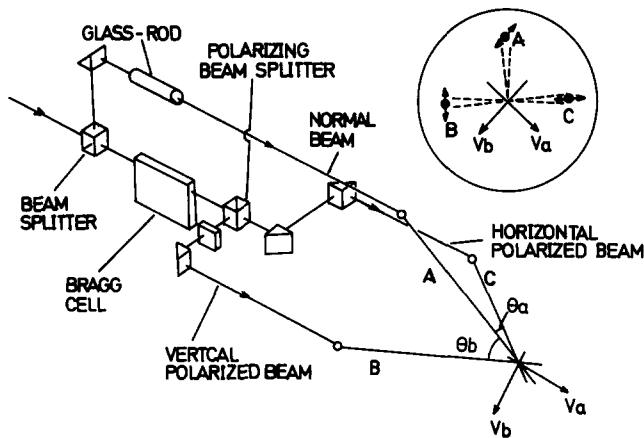


Figure 3 Optical system of laser Doppler velocimeter

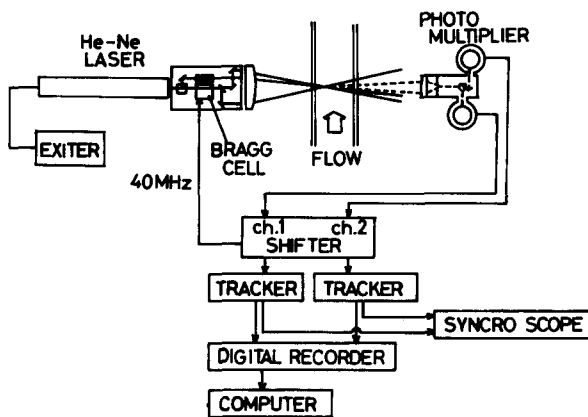


Figure 4 Processing system of laser Doppler velocimeter

was controlled so as to coincide with the local flow velocity so that the flow field to be visualized was not seriously disturbed. Streak lines were photographed by making use of a video camera and were studied later by replaying the video tape. Sketches to be shown later were reproduced from the replayed video pictures.

Simultaneous measurement of two velocity components, normal and streamwise, was made with a one-color, three-beam laser Doppler velocimeter at five streamwise positions of $x/H = 1.5, 2.5, 3.5, 5.5,$ and 9.5 . To secure the necessary density of scattering particles, a small amount (about 10^{-6} volume fraction) of commercial white poster paint was mixed into the water that was circulating in the channel. The optical arrangement used in the present study is schematically shown in Figure 3. A He-Ne laser beam was first separated into two beams with a splitter. A 40-MHz optical frequency shift was applied to one of them by making use of Bragg cell in order to make the detection of flow direction in the recirculating flow region possible. Orthogonal polarization and separation into two more beams from the frequency-shifted beam was made with a polarization separator. Modification of polarization from linear to elliptic after passing through an acrylic wall reported elsewhere¹⁰ was checked not to be serious at every measuring point. Electronic frequency shift-down was applied to the output signal from the photomultiplier in order to keep the frequency range suitable to secure a high signal-to-noise ratio for the output of frequency tracker (Figure 4). The values of two velocity components V_a and V_b , illustrated in Figure 3 are related to the Doppler shift frequencies, f_{DH} and f_{DV} , respectively,

obtained for the two polarized beams orthogonal to each other as follows:

$$V_a = \frac{(f_{DH} - f_0)a}{2 \sin\left(\frac{\theta_a}{2}\right)} \quad (2)$$

$$V_b = \frac{(f_{DV} - f_0)a}{2 \sin\left(\frac{\theta_b}{2}\right)} \quad (3)$$

where f_0 is the frequency shift given by the Bragg cell, a the wave length of the laser beam, and θ_a and θ_b , respectively, the intersection angle between beams A and C and between beams A and B. Two velocity signals were recorded on a digital magnetic tape together with the drop-out signals of both frequency trackers. Coincidence of the two signals was checked at every sampling time. When signal bursts were observed to occur in the two signals within the time span of $100 \mu s$, two velocity signals were judged to originate from the same scattering particle and were used in the data processing. The effective parts of the signals were extracted from other parts by making use of the drop-out signal in the data processing, and they were used to obtain the averaged velocity and the statistical quantities of the fluctuating velocity. Instantaneous streamwise and cross-stream velocity components U and V were obtained in the data processing from the values of V_a and V_b at every sampling time. Their averaged values and other statistical quantities of fluctuating velocity components were also obtained from data processing. The data processing was done with a FACOM VP200/400 computer at the Data Processing Center of Kyoto University.

Results and discussion

Figure 5 shows the streamwise distributions of the Nusselt number Nu_H measured for all the cases of C0, C1, C2, and C3 at three different values of Reynolds number. At any Reynolds number, some degree of heat transfer enhancement due to the insertion of cylinder is observable for the two cases of C2 and C3 in the first region after $x/H = 0$, the region of the streamwise length of several step height (the region A). Heat transfer enhancement is most effectively achieved in that region in the case C3, the case of the highest cross-stream position of cylinder. This is common to all Reynolds numbers studied. However, at the two cases of $Re = 700$ and $1,000$, the Nusselt number has a lower value than that for the undisturbed case C0 at the positions downstream of the region A. Therefore, at these Reynolds numbers, a space-mean Nusselt number averaged over the whole part of measured region is not noticeably increased due to the insertion of a cylinder. Thus, in the following, a detailed discussion is given only to the heat transfer data obtained at $Re = 1,400$, for which the Reynolds number flow visualization and velocity measurement were also made.

In the case without an insertion of a cylinder, the value of Nu_H increases after the step first gradually and next rather sharply, and it reaches a peak around $x/H = 6$. The peak position of Nu_H corresponds roughly to the flow reattachment point. This is discussed later. For the lowest case of the cylinder position C1, the distribution of Nu_H is only slightly different from that of the case C0. Therefore, an insertion of a cylinder does not lead to any noticeable enhancement of wall heat transfer at this insertion position of a cylinder. In the middle case of cylinder position C2, another peak appears in the distribution of Nu_H around a streamwise position of $x/H = 1.3$. However, enhancement of heat transfer is rather localized in

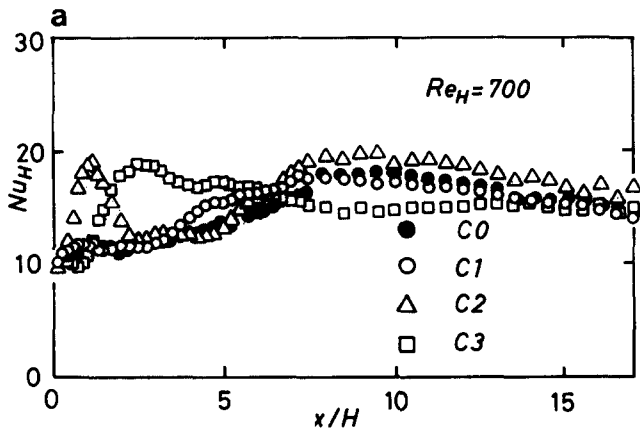


Figure 5(a) Local Nusselt number, $Re = 700$

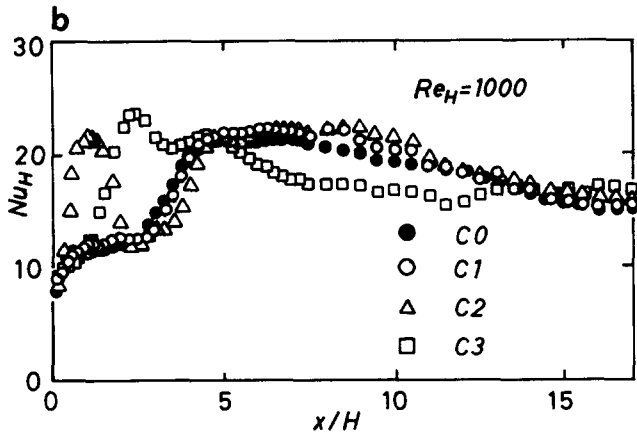


Figure 5(b) Local Nusselt number, $Re = 1,000$

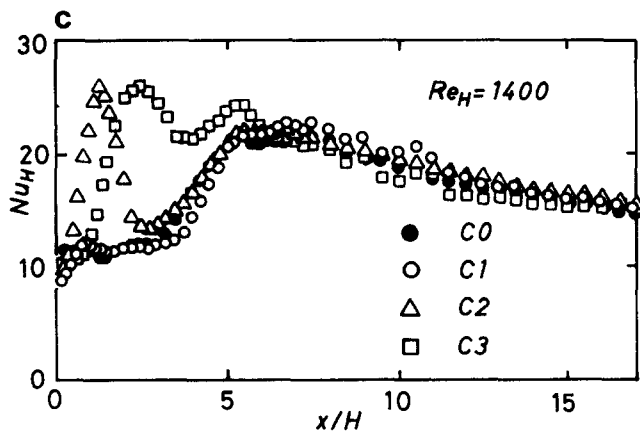


Figure 5(c) Local Nusselt number, $Re = 1,400$

this case only around this peak because the value of Nu_H decreases sharply after the peak. No significant change occurs around the main peak of Nu_H distribution. Therefore, the effect of placement of the cylinder is modest. In the case of the highest cylinder position C3, the first peak appears a little downstream from the counterpart observed in case C2 and becomes broader too. In addition to this, the main peak moves a little bit toward the upstream from the corresponding positions of the main peak of other cases. Therefore, the depression of Nu_H distribution between the first and the main peaks is shallow so that

effective enhancement of heat transfer is attained in this case by the insertion of a cylinder.

Sketches of streak lines illustrated in Figure 6 were reproduced from the video pictures. At the Reynolds number of 1,400, flow downstream of the step is transitional, i.e., unsteady but basically of a periodical nature in the case C0. Thus, the streak lines near the separation streamlines develop into wavy or vortical motion as they flow downstream. An intermittently spaced vorticity-concentration region (hereafter called discrete vortices) flows downstream and comes close to the bottom wall around at $x/H = 8$. The flow reattachment point may fluctuate to and fro from time to time but its statistically averaged position is considered not to be largely distant from $x/H = 8$ but to be a little upstream of that position, because the circulating fluid motion induced by a discrete vortex does not look very strong compared with its translational motion. The main peak of Nusselt number distribution observed in this case is mild, but it is located around $x/H = 6$, noticeably upstream of $x/H = 8$ and probably upstream of the flow reattachment point. Similar spatial separation between the Nusselt number peak position and the flow reattachment point was reported for other types of separating and reattaching flows^{11,12} even if the distance observed between the two points was not so large.

In the case C1 when the cylinder was mounted at the lowest position, the top surface of the cylinder is positioned at the same level as the top surface of the step. Thus, the flow coming from upstream of the step is not seriously obstructed by the cylinder and the dividing shear layer between the main flow and the recirculating flow region is not noticeably affected by the presence of the cylinder. Therefore, the streak lines around the separation streamline from the top corner of the step resemble in behavior the counterparts for the case C0. In the case C2, on the other hand, the top half of the cylinder is located above the top surface of the step. Thus, firstly, the motion of fluid flowing over the cylinder is affected to some extent. Related

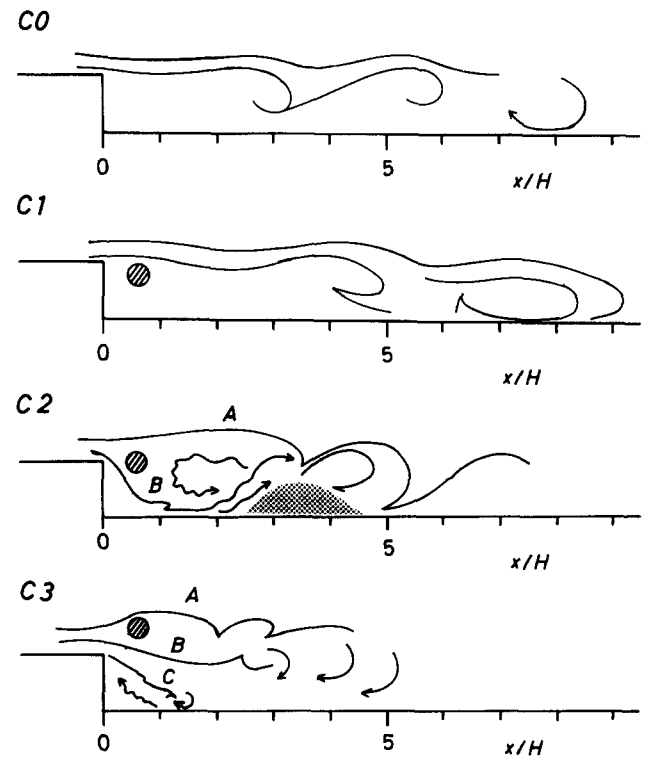


Figure 6 Sketch of flow visualization (a) without cylinder, (b) $y_c/H = 0.8$, (c) $y_c/H = 1.0$, and (d) $y_c/H = 1.5$

to this effect, the reattachment of discrete vortices sometimes occurs around $x/H = 5$, at a position a little but clearly upstream of the corresponding positions observed in the cases of C0 and C1. This is illustrated by a typical behavior of the streak line A in Figure 6c. Secondly, some portion of the fluid passing over the top of the step creeps into the region underneath the cylinder through the gap between the step and the cylinder. This is illustrated by the streak line B in the same figure. The streak line B moves down and once reattaches the bottom surface. But it separates soon from the bottom surface and is entrained into the wake of the cylinder. Therefore, a separation bubble appears downstream for the reattachment point. This is illustrated as the shaded region in the figure, which corresponds to the deeply depressed region of Nu_H , and the position of the first peak of Nu_H corresponds to the reattachment point of the streak line B. The main peak of Nu_H distribution looks a little sharper and is located a little upstream in this case than in the cases of C0 and C1. This may be related to the fact that the reattachment of the streak line A occurs at the position a little upstream from the counterpart of the cases C0 and C1. In the last case, C3, a larger amount of fluid moves through the gap between the cylinder and the top corner of the step. In the near wake behind the cylinder, the streak lines A and B drawn in Figure 6d show a behavior similar to the counterparts of the case when the cylinder is located in a uniform flow. Therefore, an alternating clockwise and counterclockwise vortical motion appears. However, after $x/H = 3$, where the streak lines become blurred and a little difficult to observe clearly, the clockwise vortical motion is still observable and surmounts the counterclockwise one. Thus, only the clockwise discrete vortices are found to reattach to the bottom surface. The streamwise position of the vortices' reattachment is almost the same as that observed for the case C2. The streak line C reattaches to the bottom surface within the spatial span between $x/H = 1.5$ and 2.5 with a noticeable level of fluctuation, which suggests the possibility that the near-wall region is disturbed by the fluctuating reattaching flow. This may be the cause for the broader first peak and the shallower depression of Nu_H distribution observed in the case C3 discussed previously.

The flow disturbance created by the insertion of a cylinder as it relates to the heat transfer characteristics is now discussed in a more quantitative manner. Figures 7a-d show the development of the averaged flow fields for the case C0 and for the three cases of C1, C2, and C3, respectively. Figures 8, 9, and 10 show the streamwise developments of cross-stream distributions, respectively, of u' and v' , the intensities of the streamwise and cross-stream fluctuating velocities, and of $-\overline{uv}$, the correlation of two fluctuating velocity components. In each figure, (a) illustrates the data for the case C0 and (b) through (d) show the data for the three cases of C1, C2, and C3, respectively. From the measured averaged velocity distributions shown in Figure 7a, the flow reattachment point is clearly located in a position between $x/H = 5.5$ and $x/H = 9.5$. In the case of C1, the averaged velocity profile is noticeably altered by the insertion of a cylinder only at $x/H = 1.5$, where the measured velocity was positive at the three points nearest to the wall. At other measuring positions, alteration of the velocity profile is minor and, even at $x/H = 1.5$, the magnitude of positive velocity near the wall is rather small. As found from the comparison among Figures 8-10, the changes in the profiles of the intensities of fluctuating velocities, u' and v' , and of the correlation $-\overline{uv}$ due to the insertion of the cylinder at this lowest position are small too. Therefore, close similarity of the distributions of Nu_H between the two cases C0 and C1 is no surprise. Figure 7c illustrates that a rather strong flow of positive velocity is generated near the wall at $x/H = 1.5$. This is related to the reattachment of the streak line B in Figure 6c. A small velocity gradient near the wall at $x/H = 2.5$ and the

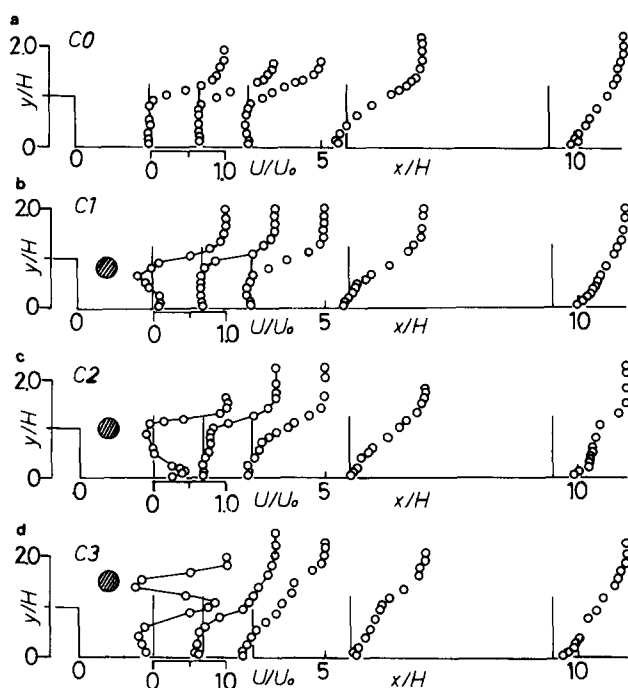


Figure 7 Averaged streamwise velocity (a) without cylinder, (b) $y_c/H = 0.8$, (c) $y_c/H = 1.0$, and (d) $y_c/H = 1.5$

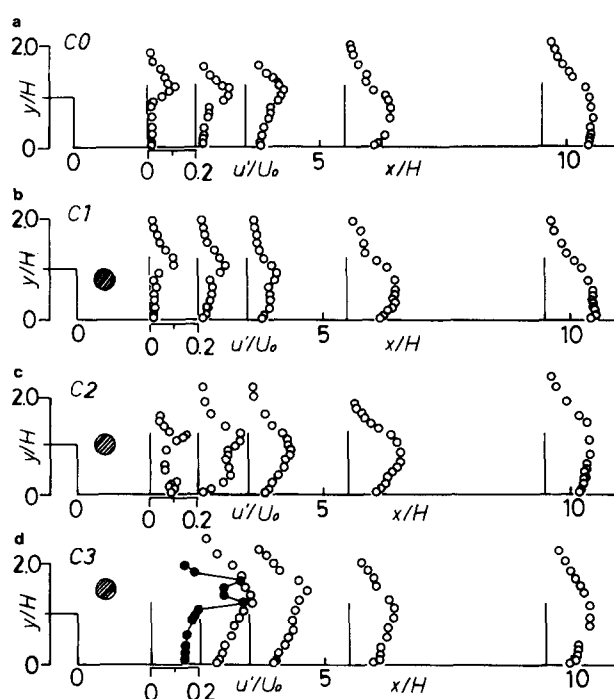


Figure 8 Intensity of streamwise velocity (a) without cylinder, (b) $y_c/H = 0.8$, (c) $y_c/H = 1.0$, and (d) $y_c/H = 1.5$

existence of backward flow near the wall at $x/H = 3.5$ confirms the flow separation after reattachment to the bottom surface and the existence of separation bubble in its downstream. Fluctuation of velocity is also intensified by the insertion of the cylinder at the middle height. The cross-stream distribution of $-\overline{uv}$ depicts a shape like the reversed one of the letter S at the first two streamwise locations. This shape is typical for the

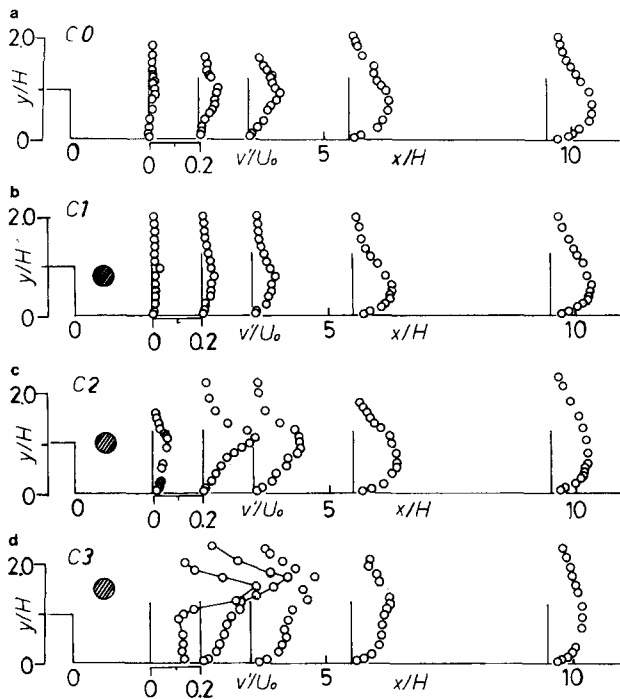


Figure 9 Intensity of normal velocity (a) without cylinder, (b) $y_c/H = 0.8$, (c) $y_c/H = 1.0$, and (d) $y_c/H = 1.5$

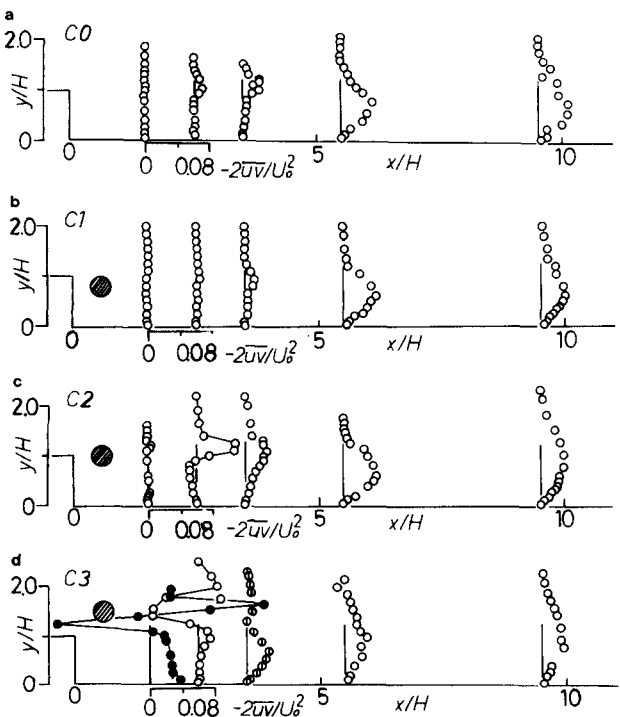


Figure 10 Cross-correlation between u and v (a) without cylinder, (b) $y_c/H = 0.8$, (c) $y_c/H = 1.0$, and (d) $y_c/H = 1.5$

wake of a cylinder located in a uniform flow. This indicates that the shear layer formed between the main flow region and the recirculating flow region is disturbed considerably. However, the intensification of the fluctuating velocity is limited only in the shear layer dividing the main flow and recirculating flow regions, and the increase of the intensities noticed there is not

big enough as compared with those of the case C3 discussed below. This is based on the fact that a deep depression exists in this case in the distribution of Nu_H between its first and main peaks.

In the last case of C3, the vertical gap between the bottom surface of the cylinder and the top surface of the step is big enough so that a certain amount of fluid can flow through it, which results in the formation of a jet-like flow around the height of the gap and in the strengthening of the recirculating flow underneath the jet-like flow. A noticeable level of backward flow velocity exists over the three streamwise positions of $x/H = 1.5, 2.5,$ and 3.5 . The cross-stream distributions of $-\bar{uv}$ at such positions are quite different from the counterparts of the other cases both in shape and magnitude. The intensities of velocity fluctuation, u' and v' , are much higher than those for other cases not only in the shear layer between the main flow and recirculating flow regions, but also in the region near the wall. These are the physical background for the broader first peak and the shallower depression of Nu_H distribution observed in this case. This further suggests that the insertion of a cylinder can be effective to alter the averaged and fluctuating velocity fields downstream of the backward-facing step, therefore, enhancing the heat transfer in that region, where the wall heat transfer is normally deteriorated. Therefore, an optimization study of the size and position of the cylinder and a similar study at larger Reynolds numbers need to be made in the future.

Concluding remarks

A study was initiated to seek to enhance the deteriorated heat transfer in a recirculating flow region downstream from a backward-facing step. The present article discussed the results of a heat transfer experiment, flow visualization, and the measurement of averaged and fluctuating velocity fields for the cases when a cylinder was mounted at three different cross-stream positions near the top corner of the step. It was demonstrated that the insertion of a cylinder is effective for altering the averaged and fluctuating velocity fields if the cylinder is located at the proper position. This change in the flow field characteristics leads to the enhancement of wall heat transfer. In the present study, the streamwise position and the size of the cylinder were kept the same for all experiments. Reynolds number was maintained rather low. Among the three cases of different Reynolds number, heat transfer enhancement was most effectively achieved at $Re = 1,400$. Similar studies at larger values of Reynolds number and optimization studies of the size and the position of the cylinder need to be made in the future.

Acknowledgment

The authors acknowledge the support of this study given through the Grant in Aid of Scientific Research of The Ministry of Education, Science and Culture, Japan, No. 63460099.

References

- 1 Goldstein, R. J., Eriksen, V. L., Olson, R. M., and Eckert, E. R. G. Laminar separation, reattachment and transition of the flow over a downstream-facing step. *J. Basic Eng.*, 1970, **92**, 732-741
- 2 Aung, W., and Goldstein, R. J. Heat transfer in separated flow downstream of a rearward-facing step. *Israel J. Tech.*, 1972, **10**, 35-41

- 3 Durst, F., Melling, A., and Whitelaw, J. H. Low Reynolds number flow over a plane symmetric sudden expansion. *J. Fluid Mech.*, 1974, **64**, 111–128
- 4 Denham, M. K., and Patrick, M. A. Laminar flow over a downstream-facing step in a two-dimensional flow channel. *Trans. Instn. Chem. Engrs.*, 1974, **52**, 361–367
- 5 Armaly, B. F., Durst, F., Pereira, J. F. C., and Shoenung, B. Experimental and theoretical investigation of backward-facing step flow. *J. Fluid Mech.*, 1983, **127**, 473–496
- 6 Seki, N., Fukusako, S., and Hirata, T. Turbulent fluctuations and heat transfer for separated flow associated with a double step at entrance to an enlarged flat duct. *J. Heat Transfer*, 1976, **96**, 583–593
- 7 Suzuki, H., Inoue, Y., Nishihara, A., and Suzuki, K. Unsteady flow and related heat transfer in a channel obstructed with a square rod—1st Rept: flow visualization and validation of numerical computation. *Trans. JSME B*, 1991, **57-536**, 1390–1395
- 8 Suzuki, H., Inoue, Y., and Suzuki, K. Unsteady flow and related heat transfer in a channel obstructed with a square rod—2nd Rept: time variation of flow pattern and statistical features of the flow. *Trans. JSME B*, 1991, **57-536**, 1396–1402
- 9 Suzuki, H., Suzuki, K., Inoue, Y., and Hagiwara, Y. Unsteady flow and related heat transfer in a channel obstructed with a square rod—3rd Rept: characteristics and mechanism of heat transfer. *Trans. JSME B*, 1991, **57-536**, 1403–1409
- 10 Suzuki, K., Abdel-Rahman, A., and Shinohara, K. A structural study of ducted turbulent flow with fluid injection from duct wall by making use of laser Doppler anemometer. *Proc. 4th Int. Symp. Application of Laser Anemometer to Fluid Mechanics*, 1988, **4**, 2.5.1–2.5.6
- 11 Kang, Y., Nishino, Y., Suzuki, K., and Sato, T. Application of flow and surface temperature visualization techniques to a study of heat transfer in recirculating flow regions. *Flow Visualization II*, W. Merzkirch, ed. 1982, 77–81
- 12 Suzuki, K., Kang, Y., Sugimoto, T., and Sato, T. Heat transfer in a circular tube downstream of an inserted orifice. *Trans. JSME B.*, 1984, **48-425**, 132–140